

# Real Image Inversion via Segments

DAVID FUTSCHIK, Czech Technical University in Prague, Faculty of Electrical Engineering

MICHAL LUKÁČ, Adobe Research

ELI SHECHTMAN, Adobe Research

DANIEL SÝKORA, Czech Technical University in Prague, Faculty of Electrical Engineering

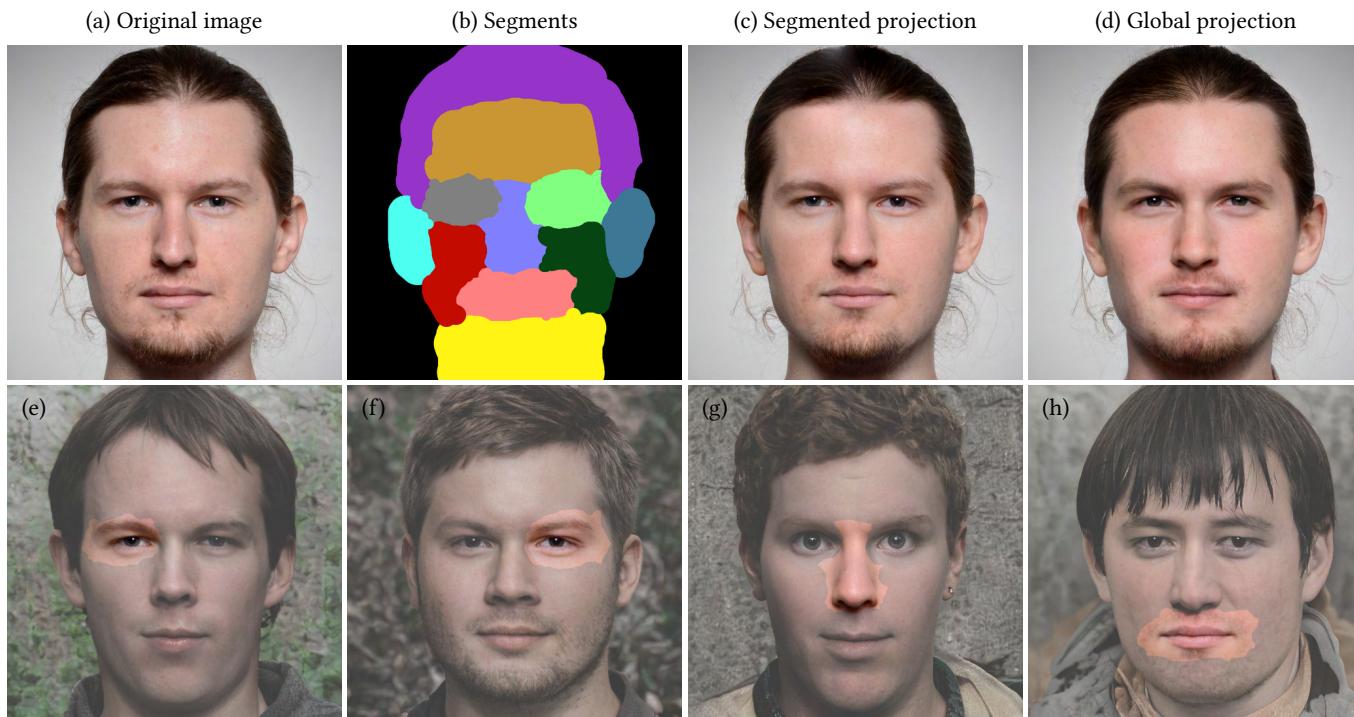


Fig. 1. A key concept of our method: The original photo (a) is subdivided into a set of segments (b) for each of which projection into a latent space is performed independently (e–h), i.e., each segment has its own latent code. Thanks to the lower number of constraints used for projection in each segment the resulting stitched image (c) preserves the identity notably better when compared to a global projection with a single latent code (d).

In this short report, we present a simple, yet effective approach to editing real images via generative adversarial networks (GAN). Unlike previous techniques, that treat all editing tasks as an operation that affects pixel values in the entire image in our approach we cut up the image into a set of smaller segments. For those segments corresponding latent codes of a generative network can be estimated with greater accuracy due to the lower number of constraints. When codes are altered by the user the content in the image is manipulated locally while the rest of it remains unaffected. Thanks to this property the final edited image better retains the original structures and thus helps to preserve natural look.

## 1 INTRODUCTION

With the increasing ability of GANs to generate images hardly distinguishable from real photographs, there have been numerous

attempts to estimate latent code of the network generating images that look very close to the given input photo. By manipulating those codes in a specific direction one may alter the appearance of the input photo in a specific way while retaining the original visual features, e.g., adding more hair to a bald person while retaining their identity.

A large body of work has been done to find an intuitive projection of latent codes into to a space in which important visual features will be disentangled so that the user can perform edits locally. Unfortunately, there is usually a trade off between the ability to get accurate reconstruction while at the same time provide an excellent disentanglement. For example in StyleGAN v2 [Karras et al. 2020], the original input code  $z \in \mathbb{R}^{512}$  is transformed into a vector  $\mathcal{W} \in \mathbb{R}^{512}$  which is easy to edit, however, difficult to estimate. While in a different approach of Karras et al. [2019]  $\mathcal{W}^+ \in \mathbb{R}^{18 \times 512}$  is used that has enough degrees of freedom to provide a good code estimation, nevertheless, it is more difficult to manipulate.

Authors' addresses: David Futschik, futschdav[at]fel.cvut.cz, Czech Technical University in Prague, Faculty of Electrical Engineering, Karlovo náměstí 13, Praha 2, Czech Republic, 121 35; Michal Lukáč, elishe[at]adobe.com, Adobe Research, 345 Park Ave, San Jose, CA, 95110; Eli Shechtman, elishe[at]adobe.com, Adobe Research, 801 N 34th St, Seattle, WA, 98103; Daniel Sýkora, sykora[at]fel.cvut.cz, Czech Technical University in Prague, Faculty of Electrical Engineering, Karlovo náměstí 13, Praha 2, Czech Republic, 121 35.

A key obstacle which stays behind this trade off is the fact that previous techniques work with the assumption that the entire image is represented by a single latent code. However, considering all pixels in the input image imposes a large number of constraints, which can make the code estimation difficult (see Fig. 1d). In our solution we relax this assumption and instead of using one single latent code, we segment the input image into a set of regions (Fig. 1b) for which we estimate local codes separately (Fig. 1e–h). Then, to reconstruct the image, we generate each segment from the corresponding latent code separately and compose the final image using those pieces (Fig. 1c).

Besides the lower number of constraints that enables estimation of latent codes that generate images closer to the input photo our segmentation-based technique also ensures precise localization of subsequent edits. Thanks to that property important visual features remain intact and thus help to retain fidelity of the original image.

The contributions of this short report are the following: (1) We demonstrate how to perform segmentation-based estimation of latent codes and how this approach can improve the ability to reconstruct important visual features in the input image. (2) We show various use cases in which precise localisation enable alternations that would be difficult to achieve using current state-of-the-art.

## 2 METHOD

### 2.1 Projection

Given a real image  $I$  and a set of segments  $S_{1,\dots,n}$  which correspond to regions in  $I$ , we perform  $n$  separate projections of  $S_n(I)$  into the desired input latent space  $X_n$ . The domain of  $X$  is not necessarily fixed. In general it can be any input space that can compactly represent inputs into the GAN. In the case of StyleGAN v2 [Karras et al. 2020], we consider  $z$ ,  $\mathcal{W}$ ,  $\mathcal{W}^+$ , and  $S$ -space [Wu et al. 2021], however, any previously published or a newly developed projection method can be used. In fact our segmented projection is a complementary improving mechanism that can help to achieve better results regardless the selected projection method (see Fig. 2). Those can possibly be even mixed to achieve best results.

The function of  $S(I)$  depends on the method which provides the input based on  $I$ . In the case of gradient descent on some image loss  $\mathcal{L}$ ,  $S(I)$  can be a composition of functions which combine the region of interest defined by  $S_k$  with  $I$  such that per-pixel loss outside the region is equal to 0. If we want to use a feed-forward code estimation, we provide the mask as a part of the input and alter the training regime of the code-providing network.

To minimize seams between individual projected segments we dilate their boundaries to achieve spatial overlap. Alternatively we can condition the projection loss so that it considers also a small neighborhood around each segment. When there are areas that we do not wish to edit at all, we exclude them from the projection altogether and in the final composition we will substitute them back directly from  $I$ .

To achieve even better inversion, we can further fine tune the underlying model for each segment separately using state-of-the-art techniques such as Pivotal Tuning [Roich et al. 2021] (see Fig. 3). Like in the projection task, fine tuning is made considerably easier

with reduced number of constraints offered by only considering the region of interest.

### 2.2 Editing

Once the projection is ready, we can perform latent space edits to achieve natural-looking changes in the input image. To achieve best results, we prepare  $S$  to follow semantic segmentation, i.e., segments containing individual facial feature (see, e.g., masks show in Fig. 1 and Fig. 2).

First type of edits we can perform are locally global, i.e., we change all segments in the same direction. For example, we can perform various  $\mathcal{W}_{edited}^k = \mathcal{W}^k + \alpha D$  changes, with known directions  $D$ , and then compose the final image using  $S$ . This type of edit can be seen in Fig. 4.

Another possibility is to perform incremental modification. In this scenario segments are optimized sequentially, edited, and the final composite becomes again a new  $I$  for the next iteration. This editing strategy is shown in Fig. 5. Such a workflow is intuitive for users as they can exactly specify what they want to change, overview the resulting composition, and then possibly go back and revise their requirements by making changes in other segments.

When making a final composition of an edited image, even when the edits are consistent in all segments global continuity is no longer guaranteed and thus a small correction is usually necessary. To this end, we employ Poisson image stitching [Pérez et al. 2003] between the segments to hide minor discrepancies.

### 2.3 Segmentation Refinement

As an improvement to the projection quality we can refine the segmentation  $S$  during the iterative optimization of  $\mathcal{W}$  or during the editing phase to avoid segment boundaries to cross salient features (see Fig. 7). To perform such a refinement we represent the boundaries of individual segments by a Level Set [Osher and Sethian 1988] and optimize them to avoid collision with areas of high difference between adjacent segments.

Let us consider an example shown in Fig. 7. Here we have an initial segmentation  $S$  that separates eyes from head. In  $S$  eyes are denoted by +1 and head by -1. The boundary between eyes and head segment is denoted as  $S = 0$  (red curve in Fig. 7c). In addition, we define a stopping function  $F = |I - I_{\mathcal{W}}|$  (see inset in Fig. 7b) where  $I$  is the original image (Fig. 7a) and  $I_{\mathcal{W}}$  is an image (Fig. 7b) generated by a latent code  $\mathcal{W}$  optimized over pixels where  $S = +1$  (interior of red curve in Fig. 7c). The Level Set method then iteratively refines  $S$  by using the following update rule:

$$S' = S + \Delta t \cdot F \cdot \|\nabla S\|,$$

where  $\Delta t$  is a small step in time (a new boundary can always be extracted by setting  $S' = 0$ ). The boundary of  $S$  moves faster at pixels  $p$  where the value of stopping function  $F(p)$  is high (yellow pixels in the inset of Fig. 7b) otherwise stays put or move slowly (blue pixels). Thanks to this property the resulting optimized boundary (Fig. 7d) avoids pixels which would otherwise introduce artifacts (Fig. 7c).

## 3 RESULTS

We test our approach on StyleGAN v2 [Karras et al. 2020] in the domain of faces, using gradient descent optimization method based

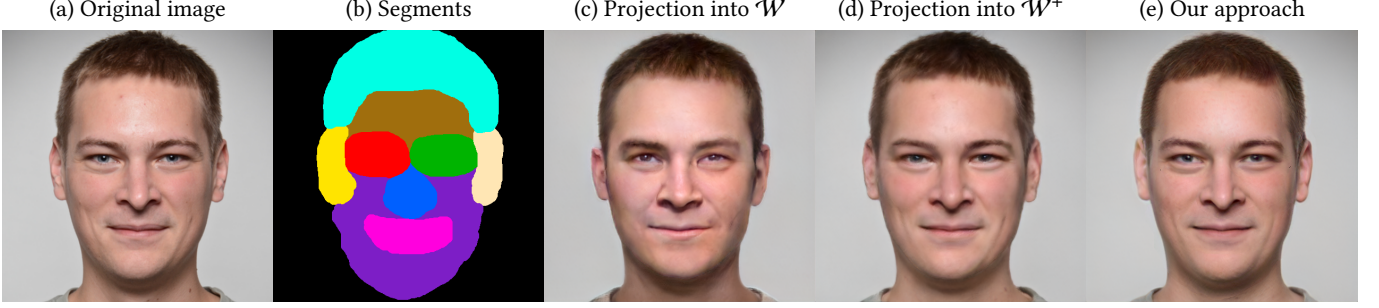


Fig. 2. Comparison of identity preservation after projecting the original photo (a) into  $\mathcal{W}$  (c),  $\mathcal{W}^+$  (d), and using our approach (e) with segments (b).

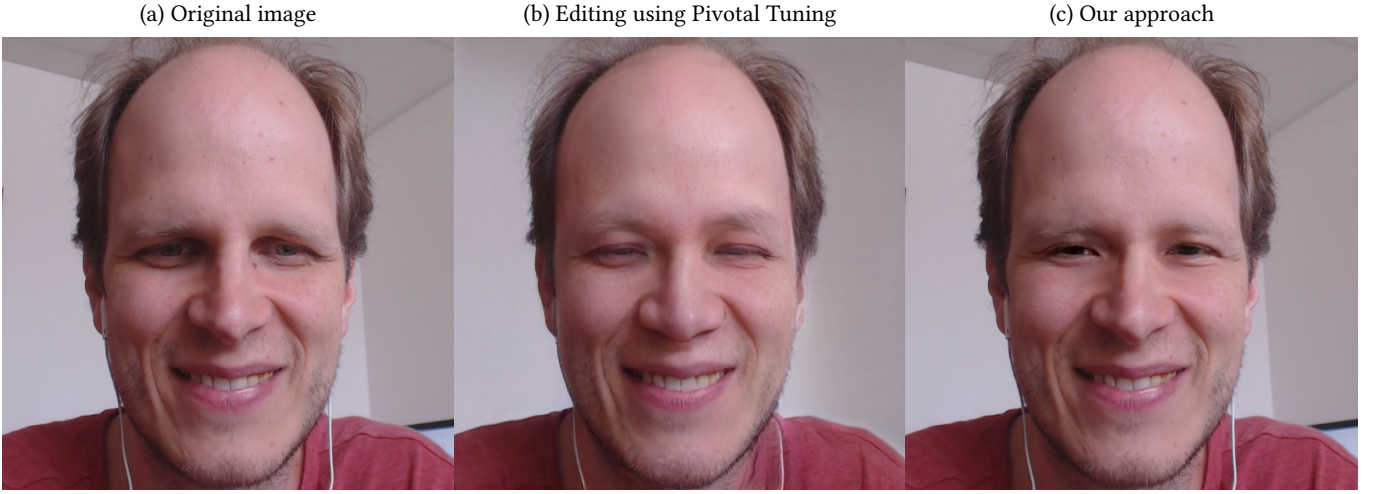


Fig. 3. Comparison of editing in  $\mathcal{S}$ -space [Wu et al. 2021] using Pivotal Tuning [Roich et al. 2021] (b) and our approach (c). Note, how even with the Pivotal Tuning and disentangled feature editing space it is still difficult to achieve good identity preservation of the original image (a).



Fig. 4. Comparison of editing in  $\mathcal{S}$ -space [Wu et al. 2021]: While changes of  $\mathcal{W}$  in  $\mathcal{S}$ -space can produce naturally looking results (b), the identity is quite far from the original image (a). Identity can be preserved notably better with  $\mathcal{W}^+$ , however, the result after performing a similar edit is not believable (c). Using our method (d) one can obtain better identity preservation as well as naturally looking edits (all segments are changed simultaneously).

on [Karras et al. 2019] to obtain the projected latent codes  $\mathcal{W}$  for each segment. Segmentation maps used in these results were hand-drawn by users who were interacting with our system. In Fig. 1, we show an example of full-face projection with eleven segments each

corresponding to a specific semantic region (e.g., eyes, hair, mouth, ears, etc.). Compared to a global projection of  $\mathcal{W}$ , we obtain an image which is much closer in identity to the original image. Moreover,



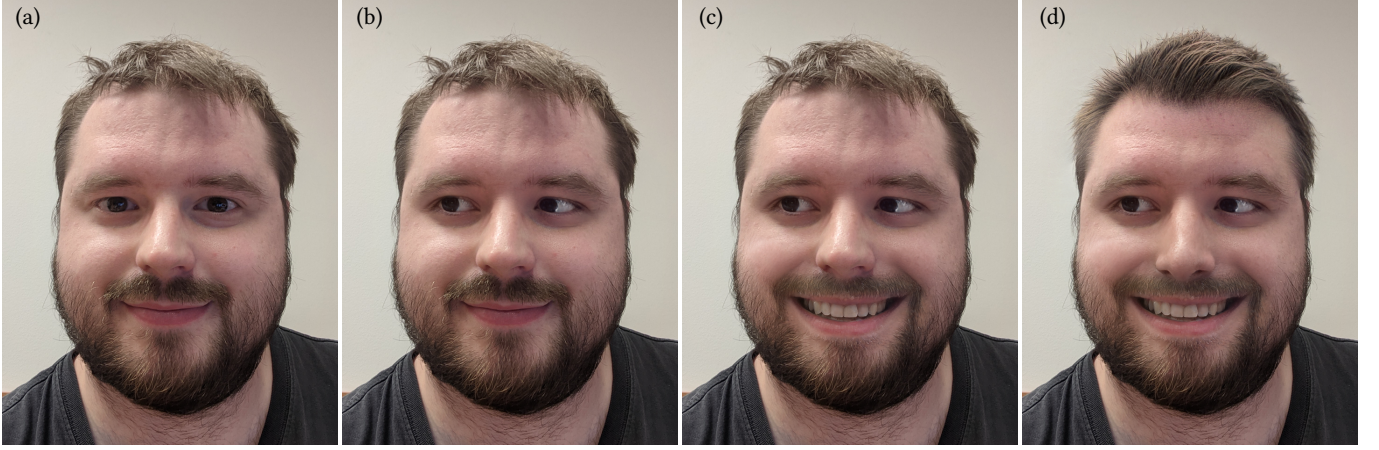


Fig. 5. Examples of local layered edits applied subsequently on a real photograph (a): changing gaze direction (b), adding smile (c), changing haircut and nose shape (d).

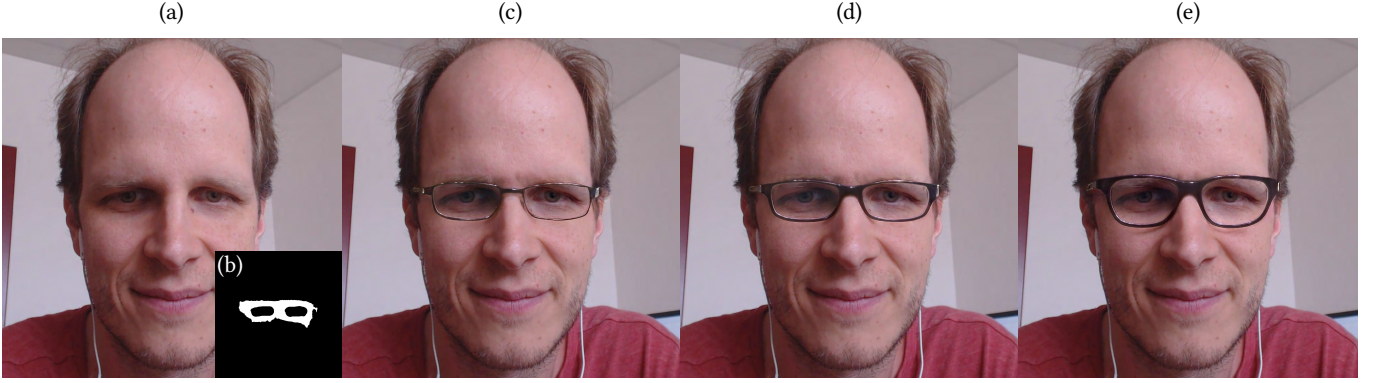


Fig. 6. Our approach (b) can achieve state-of-the-art identity preservation even for complex edits such as putting on glasses (c–e) to a subject in the original photo (a).

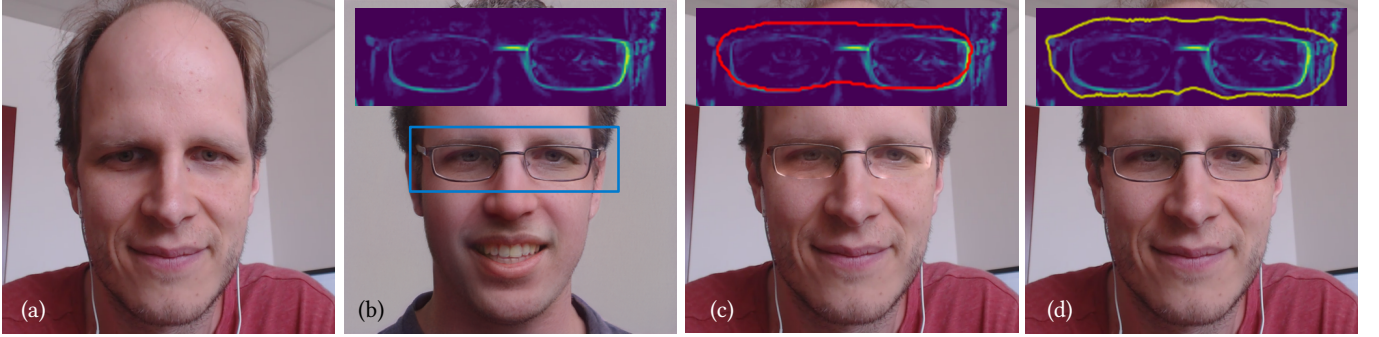


Fig. 7. An example of automatic mask refinement—our approach is applied to find and edit a latent code  $\mathcal{W}$  with the aim to add glasses to the original photo (a). For the initial projection segmentation mask  $S$  denoted by red curve in the inset of (c) was used. However, after editing boundary of  $S$  started to collide with new features in the edited image and thus the resulting composite contains artifacts (c). Automatic mask refinement (yellow curve) was used to avoid such collision and produce clean composite (d). As a stopping function  $F$  for mask refinement based on Level Set method magnitude of pixel differences between images (a) and (b) is used, see insets in figures (b–d).



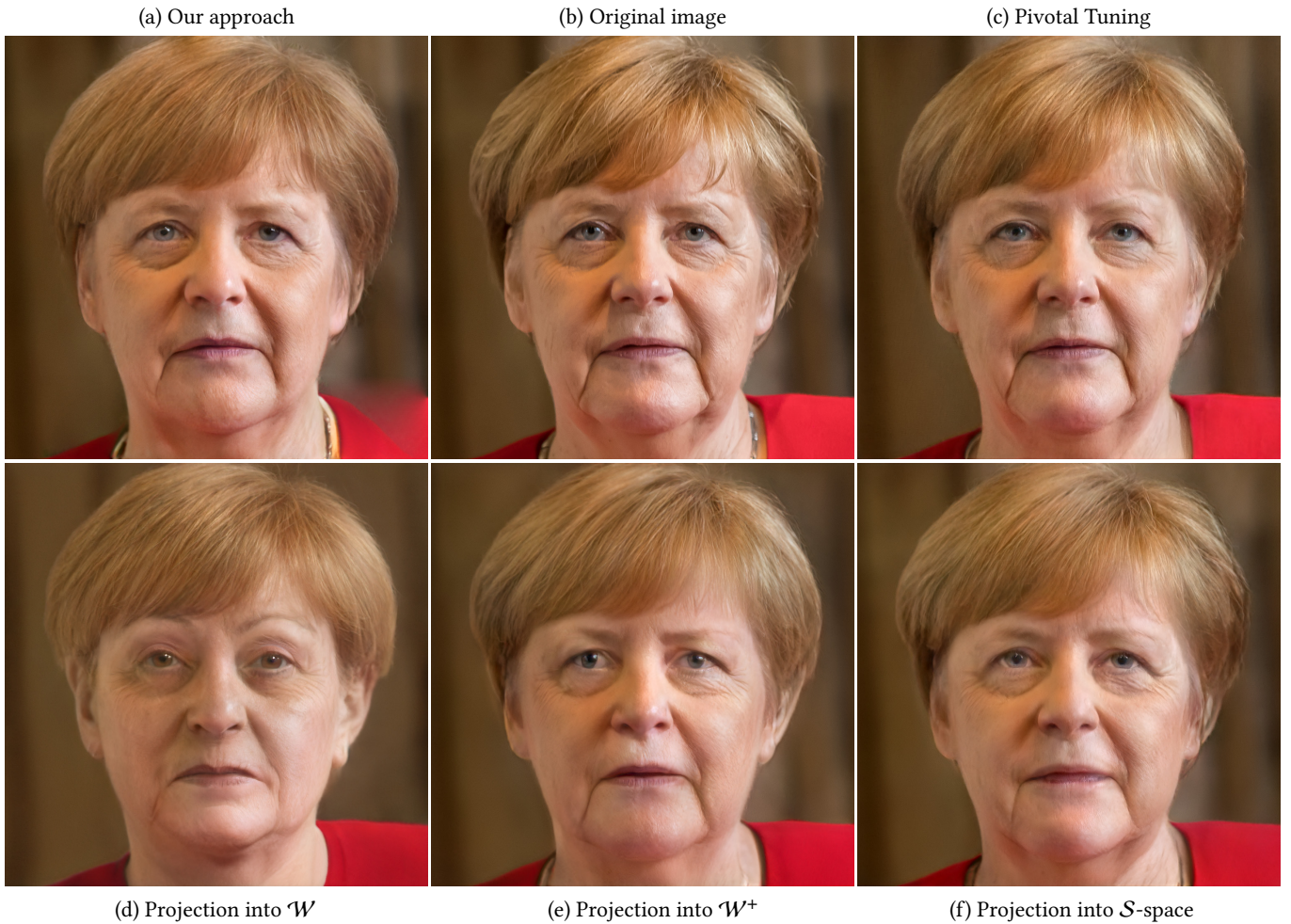


Fig. 8. An example of challenging projection task: our approach (a) used to reproduce identity of Angela Merkel in the original image (b). Although Pivotal Tuning [Roich et al. 2021] (c) achieves better identity preservation it requires custom StyleGAN v2 model. Other projections based on standard StyleGAN v2 model such as  $\mathcal{W}$  (d),  $\mathcal{W}^+$  (e), or  $\mathcal{S}$ -space [Wu et al. 2021] (f) tend to alter the identity of Angela Merkel considerably.

the segments are nicely stitched without visible seams or discontinuities. A more challenging projection result is present in Fig. 8. In this case project on  $\mathcal{W}$  (Fig. 8d),  $\mathcal{W}^+$  (Fig. 8e),  $\mathcal{S}$ -space [Wu et al. 2021] (Fig. 8f), and Pivotal Tuning [Roich et al. 2021] (Fig. 8c) were used to match the identity in the target photo (Fig. 8b). Our approach (Fig. 8a) performs substantially better than techniques which do not require custom model, i.e.,  $\mathcal{W}$  (Fig. 8d),  $\mathcal{W}^+$  (Fig. 8e), and  $\mathcal{S}$ -space (Fig. 8f). Although Pivotal Tuning achieves slightly better identity preservation than our techniques, it requires custom fine-tuned StyleGAN v2 model which can be difficult to manipulate.

In Fig. 4 we show a smile enhancement edit. While projecting into  $\mathcal{W}^+$  achieves identity on par with our projection, the result of changing the smile through a latent code manipulation in  $\mathcal{S}$ -space is far from looking realistic. Contrary,  $\mathcal{S}$ -space manipulation performed per-segment in our method retains more realism in the final image. An example of incremental editing scenario can be seen

in Fig. 5, where a user selectively draws segments to change desired attributes of a real face. First, the gaze is changed through changes in  $\mathcal{S}$ -space, then the smile is enhanced via a move in the  $\mathcal{W}$  space, and so on.

Interestingly, our method can even be applied to out-of-domain images, such as paintings in Fig. 9 where we perform changes on an artwork using a network trained exclusively on real photographs of faces. Because the segments are relatively small, the projection is still feasible and subsequent edits look convincing.

#### 4 LIMITATIONS

Despite the fact the current trend in the literature is to perform edits that have global impact on the entire image, we argue that in practice, users also often do selective, smaller edits for which our method is highly beneficial. Although, our approach supports global editing as well (by changing the latent vectors in all segments



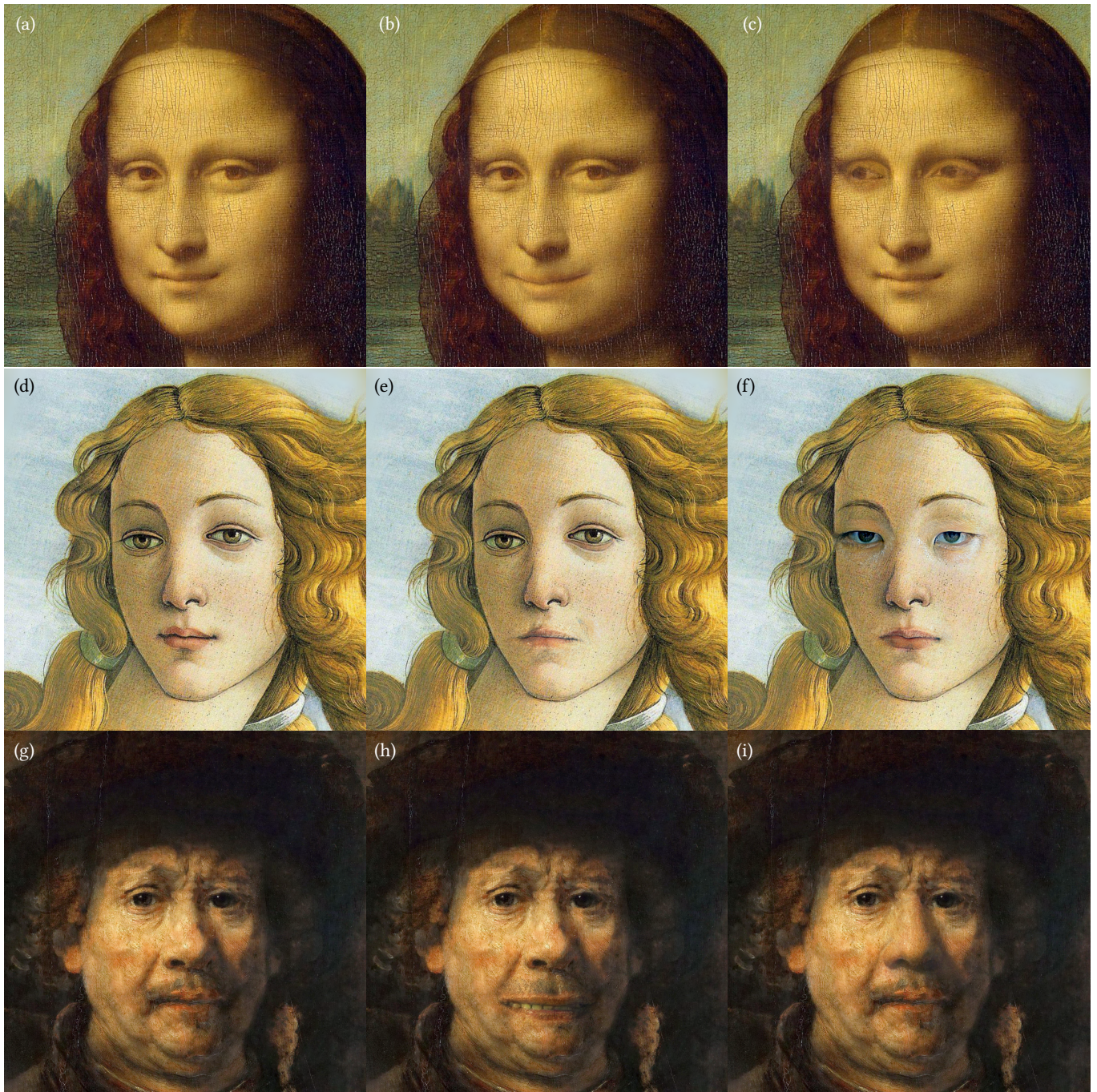


Fig. 9. Thanks to the lower number of constraints, our technique can achieve edits that would normally require StyleGAN trained on a different domain. Here, we perform edits on famous artworks using StyleGAN v2 trained solely on real faces: (a) Da Vinci’s Mona Lisa, (b) more pronounced smile, (c) change in the gaze direction, (d) Botticelli’s The Birth of Venus, (e) change in the mouth expression, (f) different shape of eyes, (g) Rembrandt’s Little Self-portrait, (h) changing mouth expression, (i) different shape of the nose.

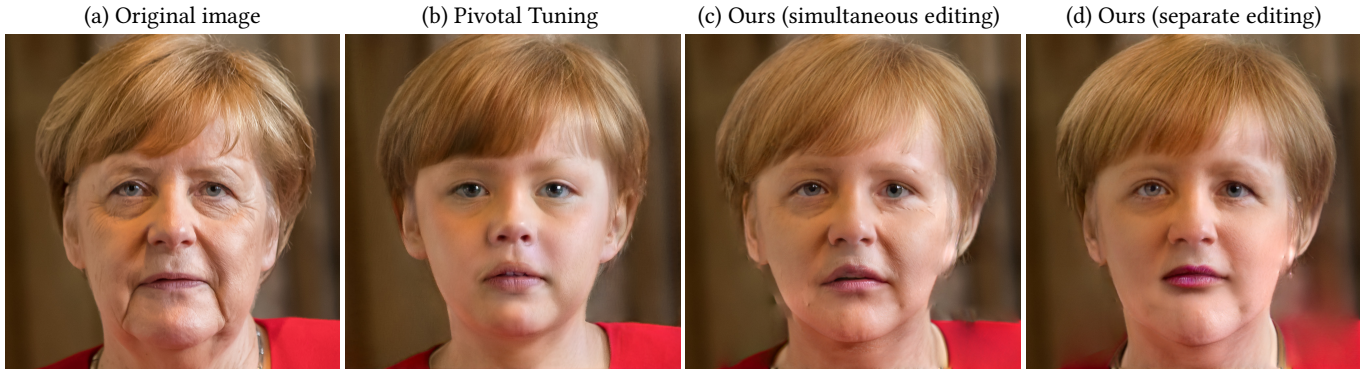


Fig. 10. Limitation—when a more dramatic edit in the latent space is applied on the original image (a), state-of-the-art global methods such as Pivotal Tuning [Roich et al. 2021] (b) would produce consistent output while our approach may introduce inconsistencies between individual segments when edited simultaneously (c). This limitation can be alleviated by editing each segment separately (d). Note, how our approach better preserves identity after editing.

simultaneously), it could encounter difficulties when the change is larger as inconsistencies between segments may become apparent (see Fig. 10c). Smaller mismatch can partially be resolved by the automatic boundary refinement discussed in Section 2.3, for more dramatic changes separate editing of latent code in each segment would yield better results (Fig. 10d).

## 5 CONCLUSION

We presented an approach to image editing based on generative adversarial networks that subdivide the input image into a set of segments for which the corresponding latent vectors are retrieved separately. In contrast to global methods that encode the entire image, our local inversion enables more accurate reconstructions, leading, e.g., to better identity preservation in facial images. We demonstrated the utility of our technique in numerous practical scenarios where previous methods may have encountered difficulties. We

believe that the complementary nature of our approach finds its application potential in modern image editing tools.

## REFERENCES

- Tero Karras, Samuli Laine, and Timo Aila. 2019. A Style-Based Generator Architecture for Generative Adversarial Networks. In *Proceedings of IEEE Conference on Computer Vision and Pattern Recognition*. 4401–4410.
- Tero Karras, Samuli Laine, Miika Aittala, Janne Hellsten, Jaakko Lehtinen, and Timo Aila. 2020. Analyzing and Improving the Image Quality of StyleGAN. In *Proceedings of IEEE Conference on Computer Vision and Pattern Recognition*. 8107–8116.
- Stanley Osher and James A. Sethian. 1988. Fronts propagating with curvature-dependent speed: Algorithms based on Hamilton-Jacobi formulations. *J. Comput. Phys.* 79, 1 (1988), 12–49.
- Patrick Pérez, Michel Gangnet, and Andrew Blake. 2003. Poisson Image Editing. 22, 3 (July 2003), 313–318. <https://doi.org/10.1145/882262.882269>
- Daniel Roich, Ron Mokady, Amit H. Bermano, and Daniel Cohen-Or. 2021. Pivotal Tuning for Latent-based Editing of Real Images. *arXiv:cs.CV/2106.05744*
- Zongze Wu, Dani Lischinski, and Eli Shechtman. 2021. StyleSpace Analysis: Disentangled Controls for StyleGAN Image Generation. In *Proceedings of IEEE Conference on Computer Vision and Pattern Recognition*. 12863–12872.